PRELIMINARY STUDY OF THE AERODYNAMIC CHARACTERISTICS OF KRUEGER FLAP ON THE SST CONFIGURATION

Dongyoun Kwak*, Keisuke Ohira**
*** Aeronautical Technology Directorate, JAXA,**
**** Engineering Solution Division, Ryoyu Systems Co., Ltd.**

Keywords: *Aerodynamics, CFD, SST, High Lift Devices*

Abstract

To improve the aerodynamic performance at take-off and landing flight and coexist with the natural laminar flow wing, the capability of the Krueger flap and its flow mechanism were investigated on a JAXA-QSST configuration. Parametric studies using numerical analysis are conducted on variation of the mutual location between the Kruger flap and main wing, and the flap deflection angle. Furthermore, the optimization by those two parameters were performed on four segments Krueger flaps. The lift-to-drag ratio characteristics are strongly influenced by the mutual locations and deflection angles by effectively controlling the vortex flow over the flaps and main wing. Comparing with the conventional leading-edge flap, higher lift-to-drag ratio is obtained by the Kruger flap. Because, the vortex lift at the flap and suppression of flow separation at main wing improve the lift-to-drag ratio by the Krueger flap deploying.

1 Introduction

Recently, civil transport aircraft is strongly requested of higher environmental performance as well as economic performance [1]. Especially, on the supersonic transport (SST), reductions of aircraft noise such as the sonic-boom at the cruise flight and the airport noise at take-off and landing flight are serious issues to realize the commercial SST [2]. The reduction of the fuel consumption is also one of key subjects to save the operation cost as well as to reduce the CO_2 emission [3].

Japan Aerospace Exploration Agency (JAXA) has been performed research on supersonic transport [4]. In this research, aerodynamic and structural integration design technologies are conducted to achieve low-noise, high aerodynamic performance, light-weight aircraft configuration. The high lift device (HLD) is one of important research subjects to improve aerodynamics at take-off and landing as well as sustain supersonic aerodynamic and noise performances.

Many research were carried out on the HLD to compensate low-speed aerodynamics [5-8]. The vortex leading-edge (LE) flap is one of suitable concepts on the highly-swept and sharped wing geometry by controlling the leading-edge separation vortex. An optimal LE flap deflection angles were obtained on 4 segment LE flaps on a QSST configuration on previously research [9]. Flow fields on the optimal deflection angle were balanced on the vortex formation over the flap and separation suppression from the LE flap hinge line. Because the separation vortex from the hinge line induces the increment of the drag as well as lift, therefore the lift-to-drag ratio becomes poor.

Recently, the Krueger flap is focused on the subsonic civil aircraft to coexist with the natural laminar flow wing [10]. Comparing with the conventional LE slat or flap, the Krueger flap system prevents from the insect contamination at take-off flight and sustains smooth surface geometry over upper surface near the LE [11].

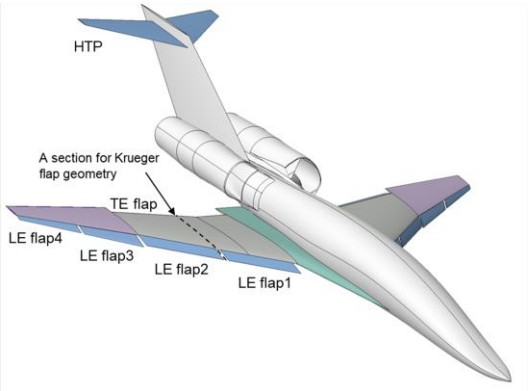

Fig.1 JAXA QSST configuration

In this research, the capability and the flow mechanism of the Krueger flap are preliminary investigated on simplified flap geometry of the highly swept SST wing. Parametric studies using numerical analysis are carried out on variation of the mutual location between the Kruger flap and main wing, and the flap deflection angle. Furthermore, the optimization by those two parameters were performed on four segments Krueger flaps.

2 QSST Configuration

Figure 1 shows a 3.2th geometry of JAXA-QSST (Quiet Supersonic Transport) configuration [12]. Total length is 47m and the cruise Mach number M=1.6. The leading-edge swept angles of the inboard/outboard wing are $\Lambda_{in}/\Lambda_{out}$=62deg/52deg. Four segments Krueger flaps were installed at the LE of the main wing, and two segments plain trailing-edge flap on inboard wing. Each segment of the Krueger flap was separate with a narrow slit to prevent the mechanically contacted each other when the flap deployed.

Details of the Krueger flap at each segment are written on Table 1. The chord length of each Krueger flap is equal with conventional single LE flap (only deflected downward direction) used in previous research to easily comparison on both [13]. It is means that the area of the Krueger flaps is equal with deflected area of the conventional LE flaps. However, the Krueger flaps are deployed from the lower surface of the main wing, therefore the wing area additionally including the Krueger flaps is 9% larger than the wing area on case of the conventional LE flap.

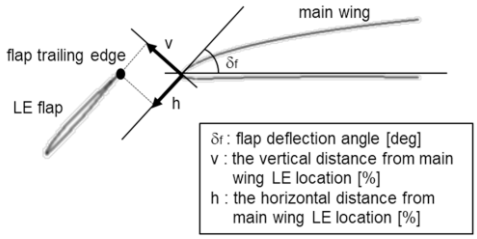

Fig.2 Details of the Krueger flap

Geometries of the flap airfoil sections were chosen as an airfoil geometry at spanwise section between LE flap1 and LE flap2 (see Fig.1).

Table.1 Details of the Krueger flaps

Krueger flap	nominal deflection angle	flap chord length	flap section geometry
LE flap1	43.1 deg	20% of the chord length at LE kink location	an airfoil geometry at spanwise section between LE flap1 and LE flap2
LE flap2	43.6 deg		
LE flap3	38.2 deg	20% of the local chord length	
LE flap4	34.1 deg		

Figure 2 shows the definition of the location of the Krueger flap from main wing. The distance, which parallels to a nominal flap deflection angles (see Table1), between the flap trailing-edge (TE) location and the LE location of main wing is defined as "*h*" which normalized using the Krueger flap chord length. As the same manner, the vertical distance between flap TE location and the main wing LE location is defined as "*v*". Nominal flap deflection angles at each segment are 5degree larger than optimal deflection angles of the conventional LE flap which obtained from the previous research [9].

3 Numerical Analysis

The flow solver used in this study is an unstructured finite volume solver FaSTAR (Fast Aerodynamic Routines) version 5.1.2-cellvertex developed by JAXA [14]. Numerical schemes used in this study are SLAU [15] for inviscid flux, GLSQ [16] for gradient reconstruction, Hishida (van Leer type) [17] for gradient limiter function and LU-SGS [18] for time advancement to solve RANS equations. Turbulence model is chosen to Spalart-Allmaras model with rotation curvature correction (SA-noft2-R) [19]. Figure 3 shows the

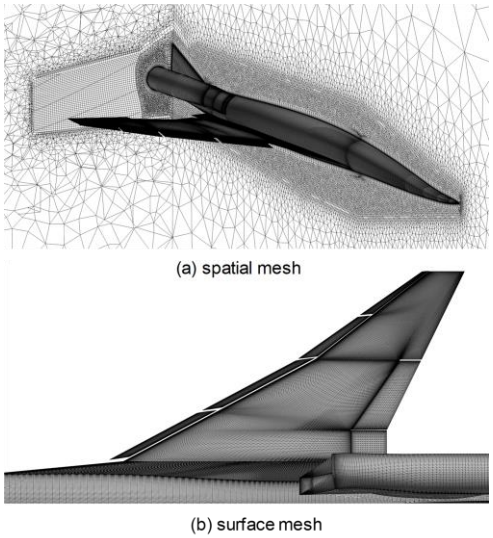

Fig.3 Computational mesh

spatial and surface mesh used in this numerical analysis. The mesh generation was carried out using commercial software "Pointwise". Total cell number is 22 million. The thickness of the first layer was 0.006mm to the normal direction, and 45layers of the prism layer were inserted. To capture to vortex flow with high fidelity, higher density mesh was installed over the upper surface. Automatic mesh generation tool named as “FlexFlap” is developed by JAXA to easily construct the mesh generation at each geometry on flap locations and deflection angles.

All CFD analysis were conducted on M=0.25, Reynolds number Re=56.6x10^6 (based on the mean aerodynamic chord length MAC=9.722m) and C_L=0.65. Furthermore, the pitching moment coefficient around the CG point kept on zero value by deflection of the horizontal tail plane at each case (C_{mCG}=0).

4 Results and Discussion

4.1 Aerodynamics of the Krueger Flap

Figure 4 shows the lift-to-drag ratio (L/D) curves on the Krueger flap deployed a typical location (h=5%, v=0%) and nominal deflection angles (rectangular symbols). The L/D-C_L curves on a clean configuration (no-flap deflection: diamond symbols) and the conventional LE flap (circle symbols) are also plotted on Fig.4. Comparing with the conventional LE flap, higher L/D is

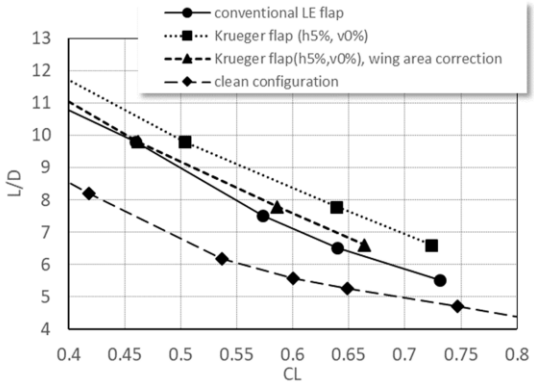

Fig.4 Comparison of the L/D-C_L curves on the conventional LE flap and the Krueger flap(C_{mCG}=0)

obtained on the Krueger flap on C_L=0.65. As mentioned above, the effective wing area on Krueger flap is 9% larger than the conventional LE flap. The triangle symbols mean a corrected L/D which normalized using the effective wing area. The corrected L/D of the Krueger flap has higher than the conventional LE flap on C_L=0.65. It means that the improvement of L/D caused by the Krueger flap is larger than the benefit by increment of wing area.

Figure 5 shows overall flow fields and static pressure distributions on the conventional LE flap and the Krueger flap. Both HLD systems deploy to nominal deflection angles and C_L=0.64. On the conventional LE flap, multiple vortices

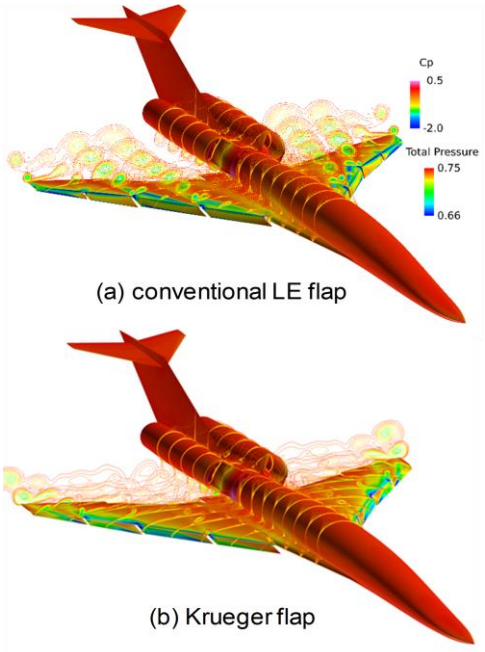

Fig.5 Static pressure distributions and total pressure distributions on C_L=0.64, C_{mCG}=0

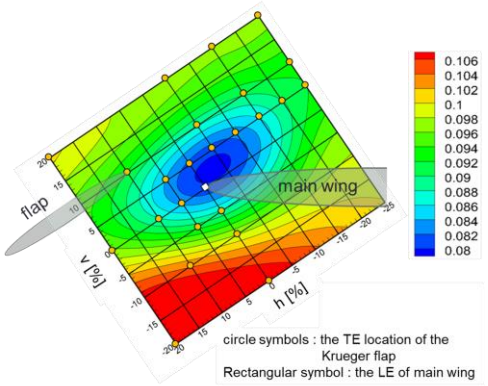

Fig.6 C_D contour when the Krueger flaps deployed to the nominal flap deflection angles (C_L=0.65, C_{mCG}=0)

are formed over the wing, and high suction regions are observed from the flap hinge line caused by LE separation vortices. However, on the case of Krueger flap, no vortices from the hinge line are observed and high suction regions are observed over flaps. It shows that the Krueger flap controls the vortical flow over the flap and main wing. In addition to effect of the wing area increment, the vortical flow controlling is additionally improve the *L*/*D*.

4.2 Flap Locations

Figure 6 shows the drag coefficient C_D contour when the Krueger flaps deployed to the nominal flap deflection angles. Cycle symbols mean the flap TE locations, as well as a rectangular symbol means the LE location of the main wing. Minimal C_D area is obtained when the flap TE locates near the upper-side of the main wing LE. The iso-C_D lines are densely at the lower-side of the main wing than the other sides. The C_D by the flap location is very sensitive at the lower direction than the upper direction or forward direction.

Figure 7 shows the surface static pressure distributions and local incidence angle distributions at mid-span section of the LE-flap1 on different vertical locations (*v*=5% and 20%). High suction regions are observed at flaps and main wing LE on *v*=5%, however high suction regions only observed at the main wing on *v*=20% (left-side on Fig.7). On local incidence angle distributions (right-side on Fig.7), high incidence angle region is observed at the flap LE on *v*=5%, on the contrary the incidence angle near the wing LE is high on *v*=20%. The LE separation vortex is formed over the Krueger flap on *v*=5%, the vortex is formed over the main wing on *v*=20%.

Flow interactions between the flap and main wing were increased when the flap moves close to the main wing (*v*=20%→5%). The incidence angle near the flap LE was increased by weaken down-wash at the flap TE which caused by the main wing. It is similar mechanism with the ground effect. Therefore, the LE separation vortices were formed over flaps. On the other hand, the incidence angle at the main wing LE was decreased by the down-wash of the Flap.

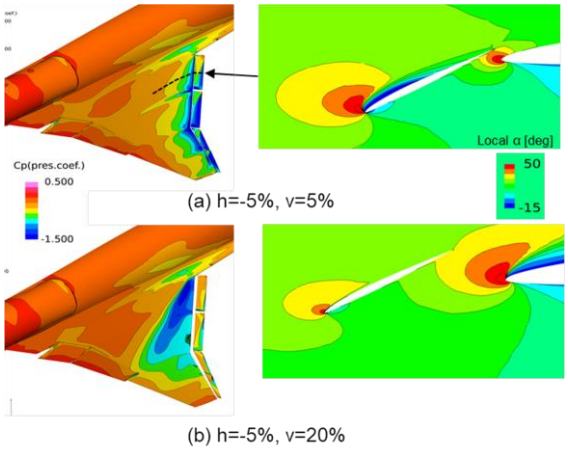

Fig.7 The Cp distributions and local incidence angle distributions at different location of the Krueger flap (left:static pressure distributions, right: local incidence angle distributions at mid-chord section of the LE-flap1)

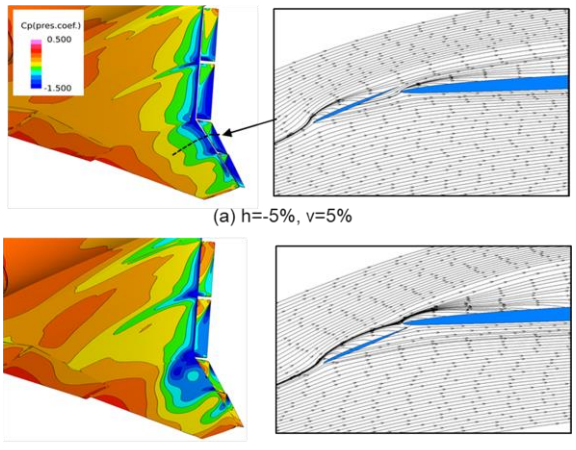

Fig.8 The Cp distributions and streamline distributions at different location of the Krueger flap (left:static pressure distributions, right: streamline distributions at mid-chord section of the LE-flap3)

Then, the flow separation and vortex formation from the wing LE was suppressed. The vortex lift on deflected flap contributes to drag reduction, and the suppression of vortex formation on the main wing restricts to increase the drag by vortex lift.

Figure 8 shows the surface static pressure distributions and streamline distributions at mid-span section of the LE-flap3 on different flap locations. The flap TE locates at upper-side of the LE of main wing on Fig.8(a), the flap TE locates at lower-side of the wing LE on Fig.8(b). When the flap locates at lower-side of the main wing, streamlines through from the flap to main wing are rapidly curved at the main wing LE. The flow over the flap is blocked by the LE geometry of main wing, and the flow separation from the main wing is promoted. High suction region is widely observed at the outboard wing on v=-5%.

When the Krueger flap deployed, vortical flow behaviors were strongly influenced by the mutual locations of the flap and main wing. Those interactions induced obvious change of the aerodynamic characteristics.

4.3 Flap Deflection Angles

Figure 9 shows C_D characteristics at several flap deflection angles. The $\Delta\delta_f$ means the difference between flap deflection angle and nominal deflection angle. Negative values of the $\Delta\delta_f$ mean the flap deflection angles are smaller than the nominal deflection angle. On the contrary, positive values mean the flap deflection angles are larger than the nominal values. Three C_D curves on different flap locations of the Krueger flap and C_D curve on conventional LE flap are also plotted on the Fig.9. With increasing the

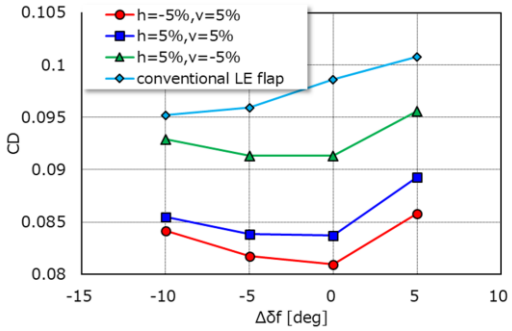

Fig.9 CD characteristics at several flap deflection angles (C_L=0.65, C_{mCG}=0)

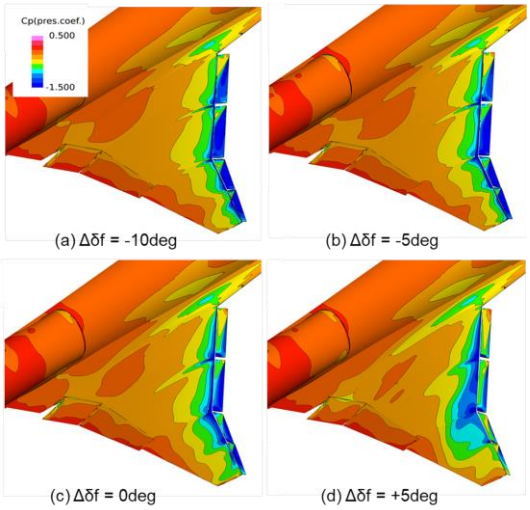

Fig.10 Static pressure distributions at several flap deflection angles of the Krueger flap

Krueger flap deflection angle ($\Delta\delta_f$=-10deg → 5deg), a minimal C_D is obtained between -5deg and 0deg on three curves. It means that C_D characteristics by flap deflection angle is not sensitive on the flap location. A flap deflection angle where a minimal C_D is obtained on the Krueger flap is different with the case on the conventional LE flap. The optimal flap deflection angle on the Krueger flap is higher than the conventional LE flap.

The vortex formation from the flap hinge line is one of reasons that causes the decrement of the L/D on the conventional LE flap. Because, when the main wing has a positive angle of attack, the vortex-lift over the wing increases not only the lift but also the drag. As a mentioned above, the flow separation and vortex formation on the main wing were suppressed by the down-wash caused by the Krueger flap. This vortex controlling effect on the main wing by the Krueger flap induces to the higher optimal flap deflection angle than the case of conventional LE flap on where flow separation will occur from the flap hinge line.

Figure 10 shows static pressure distributions at several flap deflection angles on same flap location (h=5%, v=5%). With increasing the flap deflection angle, high suction regions are shifted from the flap to main wing. The minimal C_D on the Krueger flap is significantly depended on the geometric relations on the LE swept back angle, flap deflection angle and angles of attack. The

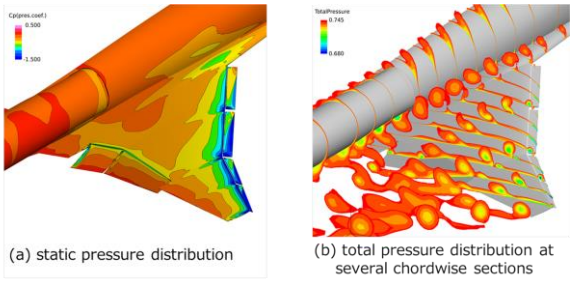

Fig.11 Overall flow fields of the Krueger flap at an optimal condition

strength of the suction force caused by the LE separation vortex and its faced direction are dominated the L/D characteristics, because the vortex suction force (vortex lift) acts to the normal direction of the surface. This is same with the concept of the LE vortex flap [5].

4.4 Optimization

Optimum design of the mutual location and the deflection angle of the Krueger flaps was conducted to understand optimal flow fields. Objective function was drag minimum at C_L=0.65, C_{mCG}=0 and the lower range than α=12.35deg. Design parameters were 5 flaps deflection angles (4 segment Krueger flap and a TE flap) and 8 locations of the Krueger flaps (vertical distance and horizontal distance from main wing LE at each 4 segments). Ranges of each parameter were chosen from the previous research [9]. Table 2 shows the optimal results obtained by the optimization. Optimal deflection angles were close to the nominal flap deflection angles by excepting the LE flap4 and TE flap. Therefore, optimal mutual locations between the flap TE and the main wing LE at each segment are located at near the center of the C_D contour shown in Fig.6.

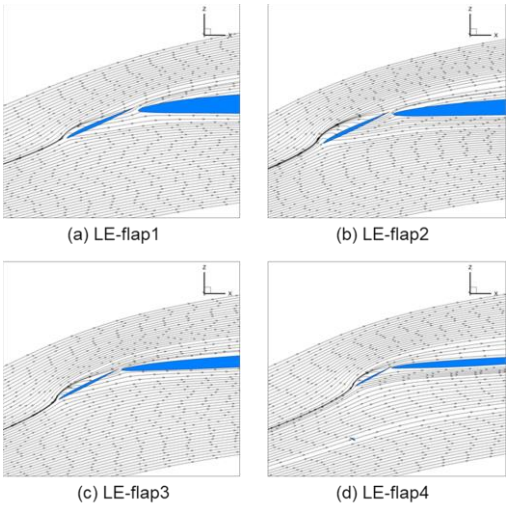

Fig.12 Streamline distributions at the mid-span section of each LE-flaps on the optimal condition.

Table 2 Optimal results of the Krueger flap

Krueger flap	nominal deflection angle[deg]	Optimal deflection angle[deg]	horizontal distance h [%]	vertical distance v [%]
LE flap1	43.1	40.3	-1.1	3.3
LE flap2	43.6	41.8	-1.2	3.1
LE flap3	38.2	38.1	0.7	2.2
LE flap4	34.1	39.5	-1.1	1.7
TE flap	8.1	16.0		

Figure 11 shows overall flow fields on an optimal condition. High suction regions are observed over the flap and near the LE of the main wing. Those high suction regions are induced by the LE separation vortices at the flap and small scaled vortices origin from the spanwise slits between each segment of the flap. However, the overall flow filed over main wing is dominated the attached flow. Figure 12 shows the streamline distributions at mid-span section on each flap segment. Smooth flow is observed between flap and main wing, and vortex is formed over the full chord length of the Krueger flap.

Figure 13 shows total pressure distributions at several chord locations on the clean configuration, the conventional LE flap and the Krueger flap. It is clearly understanding that, comparing with the cases of clean configuration and the conventional LE flap, optimal vortical flow fields are formed by the Krueger flap as that the LE separation vortices located over the flap and attached flow formed over the main wing. The L/D =8.7 at C_L=0.65 was obtained by the optimization of mutual location and deflection

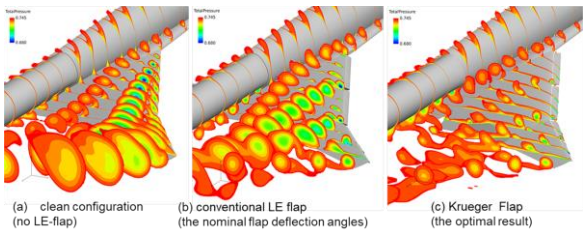

Fig.13 Total pressure distributions on three LE flap systems ((C_L=0.65, C_{mCG}=0)

angle of the Krueger flap (referred on Fig.4). Comparing with the conventional LE flap, large improvement of L/D was achieved on the optimal conditions of the Krueger flap. Which was caused by the vortical flow controlling as well as the increment of the wing area.

It is noted that though high aerodynamic capability by the Krueger flap was obtained in this study, the Krueger flap and main wing geometry were not considered the mechanical support, deploying systems and flap storing [20,21]. Further study is needed on the aerodynamic and structural issues on real geometry of the Krueger flap systems.

5 Conclusion

The capability and flow mechanism of the Krueger flap were preliminary investigated using a simplified flap geometry on SST configuration (JAXA-QSST). Parametric studies using RANS-CFD analysis were conducted on the Krueger flap with variation of the mutual locations between the flap and main wing, and the flap deflection angles. Optimization on those two parameters were also performed to understand the flow features on the optimal condition of the Krueger flap.

- When the mutual location changes between the Krueger flap and main wing, minimal C_D is obtained at the flap TE located at upper-side near the main wing LE. Interactions of the flap and main wing control the vortical flow. Flow separation and vortex formation at the main wing are suppressed by the down-wash caused by the flap, as well as the LE separation vortex formation over the flap is promoted by the main wing.
- When the Krueger flap deflection angle changes, minimal C_D is obtained at slightly higher flap deflection angle than the case of the conventional LE flap. Because the down-wash of the Krueger flap acts to suppress the flow separation on the main wing.
- Flow field on the optimal conditions shows that the LE separation vortices are formed over each segment of Krueger flaps and attached flow is formed overall of the main wing.
- The L/D on the Kruger flap is further improved than the conventional LE flap. Comparing with the conventional LE flap, improvement of the L/D by the Krueger flap is larger than the effect of wing area increments by Krueger flap deploy.

Acknowledgement

These calculations were performed on JAXA Supercomputer System generation 2 (JSS2).

References

[1] Dickson, N., ICAO Noise Standards, ICAO Symposium on Aviation and Climate Change, “Destination Green”, Montreal, Canada, 2013.

[2] Kubota, H., Technological and Environmental Issues for Accomplishment of Supersonic Transport, Proc. JSASS 16th International Session in 40th Aircraft Symposium, pp. 5-8, 2002.

[3] Green, J.E., Civil Aviation and the Environmental Challenge, The aeronautical journal, 2003.

[4] Aeronautical Technology Directorate, JAXA, http://www.aero.jaxa.jp/research/frontier/sst/.

[5] Rinoie, K., Stollery, J. L., Experimental Studies of Vortex Flaps and Vortex Plates, Journal of Aircraft, Vol.31, No.2, 1994, pp. 322-329.

[6] Buchholz, M.D., and Tso, J., Lift Augmentation on Delta Wing with Leading-Edge Fences and Gurney Flap, Journal of Aircraft, Vol.37, No.6, 2000, pp.1050-1057.

[7] Kuo, C. H., Hsu, C.W., Development of Vortical Structure over Delta Wing with Leading-Edge Flap, Journal of Aircraft, Vol.34, No.5, 1997, pp.577-584.

[8] Lei, Z., Kwak, D., Higuchi, K. and Rinoie, K., Experimental Investigation of a Segmented Flap System of a Cranked-Arrow Wing, Transactions of the Japan Society for Aeronautical and Space Sciences, Vol.55, No.5, pp.304-312, 2012.

[9] Ohira, K. and Kwak, D., Optimum Design of the Leading edge / Trailing edge Flaps on the Supersonic Transport, 53th Aircarft Symposium, JSASS-2015-5080, 2015(in Japanese).

[10] Koeing, J, Fol, T. and Kierbel, D, Clean Sky SFWA: Preparation of the Airbus A340-300 BLADE Natural Laminar Wing Flight Test Demonstrator, 7th European Aeronautics Days, London, 2015.

[11] Tamigniaux, T.L.B., Stark, S.E. and Brune, G.W., An Experimental Investigation of the Insect Shielding Effectiveness of a Krueger Flap/Wing Airfoil Configuration, AIAA Paper 1987-2615.

[12] Ueno, A., Watanabe, Y., El Din, S.I., Grenon, R. and Carrier, G., Low Boom/Low Drag Small Size Supersonic Aircraft Design, ECCOMAS2016, Greece.

[13] Ohira, K., and Kwak, D., Investigation of Turbulence Models for the Supersonic Transport Configuration at Low-speed and High Alpha Flight Condition, AIAA Paper 2014-3098, 2014.

[14] Hashimoto A., Murakami K., Aoyama T., Ishiko K., Hishida M., Sakashita M., Lahur P. R. Toward the Fastest Unstructured CFD Code "FaSTAR".AIAA-paper 2012-1075, 2012.

[15] Shima, E. and Kitamura, K. Parameter-Free Simple Low-Dissipation AUSM-Family Scheme for All Speeds. AIAA Journal, Vol. 49, No.8, August 2011, pp.1693-1709.

[16] Shima, E., Kitamura, K., Haga, T., Green-Gauss/ Weighted-Least-Squares Hybrid Gradient Reconstruction for Arbitrary Polyhedra Unstructured Grid, AIAA Journal, Vol.51, No.11, 2013, pp.2740-2747.

[17] Hishida, M., Hashimoto, A., Murakami, K., Aoyama, T. A new slope limiter for fast unstructured CFD solver FaSTAR. JAXA-SP-10-012, 2011, pp. 85-90 (in Japanese).

[18] Men'shov, I., and Nakamura, Y. Implementation of the LU-SGS Method for an Arbitrary Finite Volume Discretization. 9th Japanese Symposium on CFD, Tokyo, Japan, 1995, pp. 123-124.

[19] Langley Research Center Turbulence Modeling Resource, https://turbmodels.larc.nasa.gov

[20] Moffitt, N. J., Badcock, D.A., Kreitzman, J. and Cheng, R., Two Approaches to Resolving the Flow Physics of a Krueger Falp for CFD/CAA Analysis, AIAA Paper 2017-3366.

[21] Akaydin, H. D., Housman, J.A, Kiris, C.C., Bahr, C.J., Hutcheson, F.V. : Computational Design of a Krueger Flap Targeting Conventional Slat Aerodynamics, AIAA Paper 2016-2958, 2016.

Copyright Statement